Multi-Dimensional Biomedical Image De-Noising Using Haar Transform

ICT PRAGUE

Eva Hošťálková, Oldřich Vyšata, Aleš Procházka

Thanks to Research grant No. MSM 6046137306

Institute of Chemical Technology in Prague, The Czech Republic
Dept of Computing and Control Engineering
Phone: +420 220 444 198, Web: dsp.vscht.cz
Email: Eva.Hostalkova@vscht.cz, Vysata@neurol.cz, A.Prochazka@ieee.org

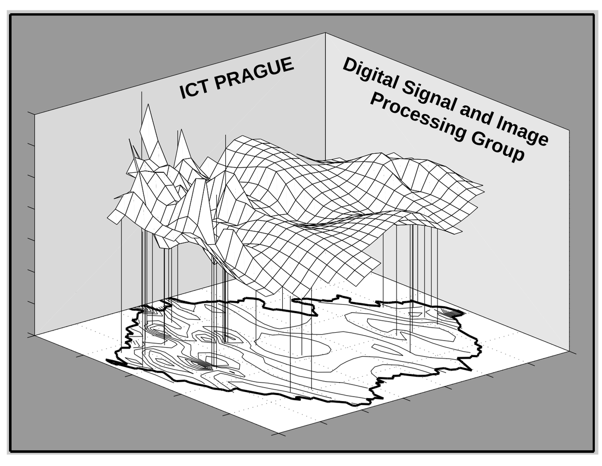

Abstract

Image de-noising and enhancement form two fundamental problems in many engineering and biomedical applications. The paper is devoted to the study of the multiresolution approach to this topic employing the Haar wavelet transform and its application to processing of volumetric magnetic resonance image sets corrupted with additional noise. The resulting coefficients are thresholded and exploited for subsequent reconstruction. The Haar transform is evaluated using both a two-dimensional approach applied individually to each image layer, and a three-dimensional technique performed on the image volume as a whole. In noise reduction, the latter approach profits from similarities between the neighbouring image layers and shows a considerable improvement over the former method. As an alternative to the wavelet transform, we also employ the Fourier transform for noise reduction by the means of spectral subtraction. The results are presented in numerical and graphical forms using three-dimensional visualization tools.

Introduction

Fundamental problems of image processing:

- Rejection of undesirable parts [8, 10]
- Feature extraction and classification
- Restoration of missing or corrupted components
- Image resolution enhancement [1], processing and coding [5]

The Haar transform (HT):

- The discrete wavelet transform [2, 7] using the Haar function
- In this paper - de-noising of biomedical magnetic resonance (MR) images by thresholding of their coefficients
- Image set decomposition:
  - Whole image volume (3-dimensional HT) [6]
  - Slice-by-slice (2-dimensional HT)

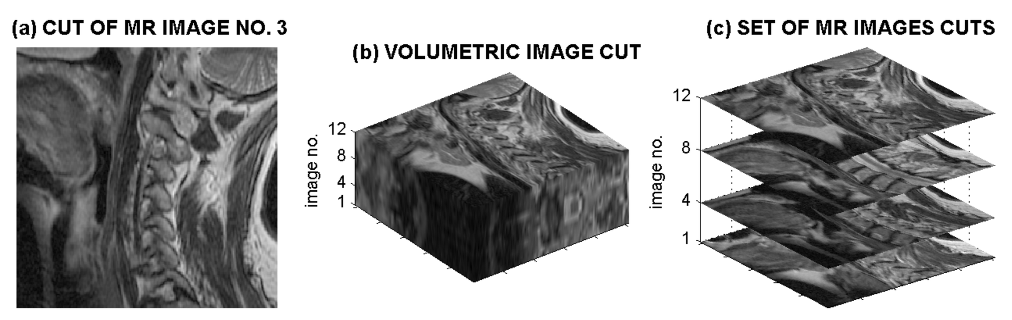

Fig. 1. Real data standing for **(a)** a selected spinal MR image, **(b)** the image volume of MR data set no. 3, and **(c)** four chosen slices of this data set

HT in Signal Analysis

The Haar transform is the simplest compression algorithm [4].

Let us have a signal $\{x(n)\}_{n=1}^{N}$. Each couple of its subsequent values $\{x(n), x(n+1)\}$ for $n = 1, 3, \dots, N-1$ and N even can be decomposed into two values

$$\begin{pmatrix} X_n \\ X_{n+1} \end{pmatrix} = \mathbf{T} \begin{pmatrix} x_n \\ x_{n+1} \end{pmatrix}, \text{ where } \mathbf{T} = \frac{1}{\sqrt{2}} \begin{pmatrix} 1 & 1 \\ 1 & -1 \end{pmatrix} \quad (1)$$

$\{X_1, X_3, \dots, X_{N-1}\}$ … the low-pass decomposition sequence
$\{X_2, X_4, \dots, X_N\}$ … the complementary high-pass sequence

This may be also expressed as:

$$\begin{pmatrix} X_1 \\ X_2 \\ X_3 \\ \cdots \\ X_N \end{pmatrix} = \frac{1}{\sqrt{2}} \begin{pmatrix} 1 & 1 & 0 & 0 & 0 \cdots & 0 & 0 \\ 1 & -1 & 0 & 0 & 0 \cdots & 0 & 0 \\ 0 & 0 & 1 & 1 & 0 \cdots & 0 & 0 \\ 0 & 0 & 1 & -1 & 0 \cdots & 0 & 0 \\ & & & & \cdots & & \\ 0 & 0 & 0 & 0 & 0 \cdots & 1 & 1 \\ 0 & 0 & 0 & 0 & 0 \cdots & 1 & -1 \end{pmatrix} \begin{pmatrix} x_1 \\ x_2 \\ x_3 \\ \cdots \\ x_N \end{pmatrix} \quad (2)$$

HT in Image Analysis

Let us have an image $[g(n,m)]_{N,M}$. For $n = 1, 3, \cdots, N-1$, $m = 1, 3, \cdots, M-1$, and N, M even, each elementary decomposition element may be decomposed

1. column-wise

$$\begin{pmatrix} G1_{n,m} & G1_{n,m+1} \\ G1_{n+1,m} & G1_{n+1,m+1} \end{pmatrix} = \mathbf{T} \begin{pmatrix} g_{n,m} & g_{n,m+1} \\ g_{n+1,m} & g_{n+1,m+1} \end{pmatrix} \quad (3)$$

2. row-wise to produce the decomposition matrix G:

$$\begin{pmatrix} G_{n,m} & G_{n,m+1} \\ G_{n+1,m} & G_{n+1,m+1} \end{pmatrix} = \begin{pmatrix} G1_{n,m} & G1_{n,m+1} \\ G1_{n+1,m} & G1_{n+1,m+1} \end{pmatrix} \mathbf{T}^T \quad (4)$$

The elements of G may be rearranged to define four submatrices. The low/low-pass submatrix defined hereby can be used for the next level of decomposition.

$$\begin{pmatrix} G_{1,1} & G_{1,3} & \cdots & G_{1,M-1} \\ G_{3,1} & G_{3,3} & \cdots & G_{3,M-1} \\ & & \cdots & \\ G_{N-1,1} & G_{N-1,3} & \cdots & G_{N-1,M-1} \end{pmatrix} \quad (5)$$

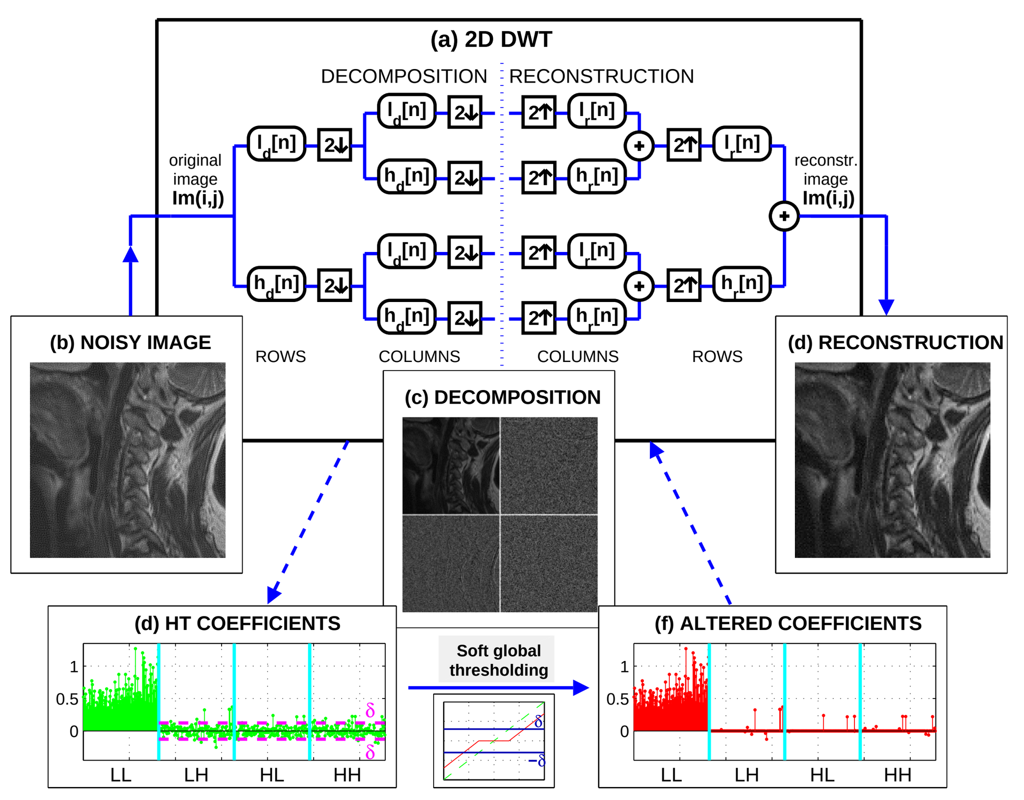

Fig. 2. HT image enhancement by thresholding of the HT coefficients displaying **(a)** the two-dimensional subband coding scheme, **(b)** the MR image with additional noise, **(c)** one-level HT decomposition, **(d)** the reconstructed image, **(e)** the decomposition coefficients, and **(f)** the thresholded coefficients utilized for reconstruction

HT in Volume Analysis

The 3-D HT is computed by adding another axis in the layer direction. That means that the outcomes of the 2-D transform of the image layers with a corresponding x,y-location are decomposed in the between-slice direction in the same way as 1-D signals [3, 4].

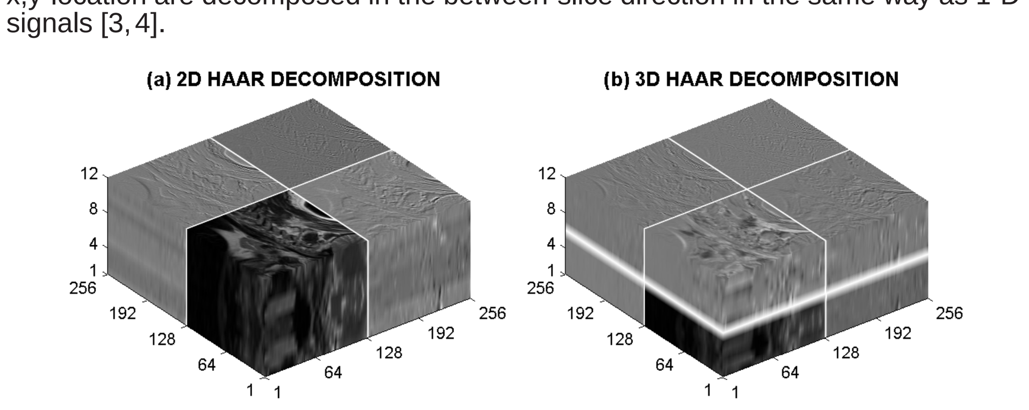

Fig. 3. Decomposition of the MR image volume presenting **(a)** 2-D slice-by-slice Haar wavelet decomposition **(b)** 3-D volumetric Haar wavelet decomposition

Threshold Selection

Soft-thresholding:

- Image de-nosing by thresholding of the HT coefficients
- The thresholded coefficients $\overline{c}(k)$:

$$\overline{c}(k) = \begin{cases} \text{sign } c(k)\ (|c(k)| - \delta) & \text{if } |c(k)| > \delta \\ 0 & \text{if } |c(k)| \le \delta \end{cases} \quad (6)$$

where $c(k)$ are the original coefficients and δ is the threshold limit

Threshold level estimation:

- The interval of threshold values: between the minimum and the maximum of the absolute value of the detail decomposition coefficients
- The optimal threshold value - the highest PSNR of the reconstructed image
- The peak signal to noise ratio (PSNR) in decibels (dB):

$$PSNR = 20 \cdot log_{10} \left(\frac{max\{g(n,m)\}}{\sqrt{MSE}} \right) \quad (7)$$

$max\{g_{n,m}\}$ … the maximum pixel value of the image $g(n,m)$
MSE … the mean square error between the original and the de-noised image volume, normalized to the number of pixels

- 2-D de-nosing: different threshold limit for each image layer
- 3-D de-nosing: a single threshold value for the whole volume

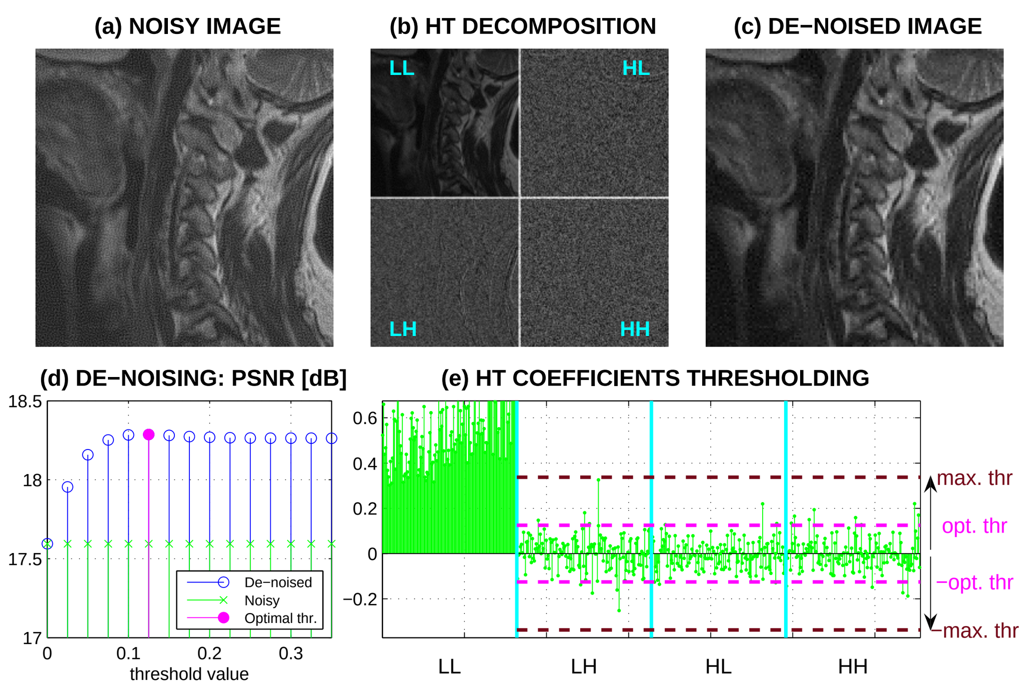

Fig. 4. 2-D processing of spinal MR image number 3 presenting **(a)** the image with additional high frequency band noise, **(b)** one-level HT decomposition, **(c)** the de-noised image reconstructed from the coefficients altered by the optimal threshold value, **(d)** the effect of threshold limit selection on the PSNR measure in decibels, and **(e)** the HT coefficients of the noisy image and the threshold levels interval

Data Specification

The following study is devoted to the problem of noise rejection in real MR images outlined in Table 1. For illustration, Fig. 1 shows set 3 composed of 12 layers with the resolution of 256 x 256 pixels.

Table 1. MRI DATA SETS SPECIFICATIONS

MRI Set	*Data Type*	*Pixel Spacing [mm]*	*Slice Spacing [mm]*	*Block Size [mm]*
1	Spine - Sagittal	0.4687	4	512 x 512 x 12
2	Spine - Axial	0.3906	4	512 x 512 x 26
3	Cut of Set 1	0.4687	4	256 x 256 x 12
4	Cut of Set 2	0.3906	4	256 x 256 x 26
5	Brain - Axial	0.4688	1	256 x 256 x 12

Results of MR Volumes De-Noising

Experiment specification:

- Ten 2-D and ten 3-D de-noising experiments for each of the five sets of MR data
- Each time with a different additional noise component

Experiment 1:

- High frequency band noise: random noise with its low frequency spectral components removed in the frequency domain
- The overall average improvement of the PSNR:
  - 2-D approach: 35.5%, 3-D approach: 54.4%

Experiment 2:

- Random noise
- The overall average improvement of the PSNR:
  - 2-D approach: 8.3%, 3-D approach: 30.5%

Results:

- The space information improves the de-noising results (see Fig. 5)
- For random noise - the layer-by-layer technique proves insufficient

Table 2. COMPARISON OF THE DE-NOISING RESULTS FOR THE 2-D AND 3-D HAAR TRANSFORM FOR RANDOM NOISE

Method / Measure		*MRI Set*				
		1	*2*	*3*	*4*	*5*
2D	*Mean PSNR [dB]*	15.7	16.4	17.4	17.5	17.1
	Improvement [%]	5.8	7.8	8.5	11.4	7.9
3D	*Mean PSNR [dB]*	18.1	20.4	19.4	21.4	22.1
	Improvement [%]	21.9	33.9	21.0	36.1	39.5

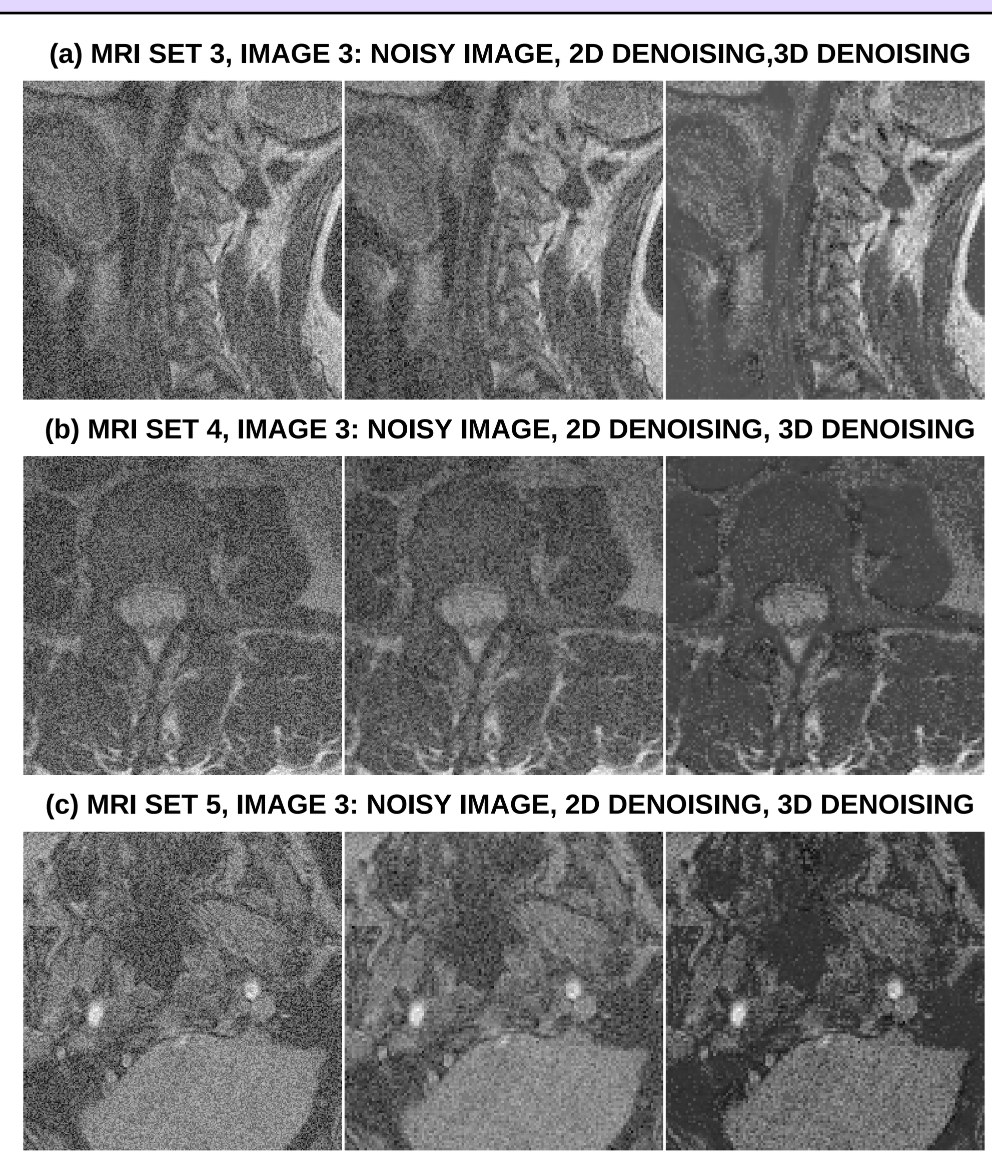

Fig. 5. Additional random noise reduction by thresholding of the 2D and 3D Haar coefficients for **(a)** image number 3 of MRI set 3 (sagittal spine), **(b)** image number 3 of MRI set 4 (axial spine), and **(c)** image number 3 of MRI set 5 (axial brain)

Spectral Subtraction

Spectral subtraction procedure:

1. One image cut and four background cuts (see Fig. 6)
2. Noise: the inverse Fourier transform (FT) of the average computed from the FTs of the background cuts
3. Noise addition in the time domain:

$$x_{n,m} = g_{n,m} + d_{n,m} \quad (8)$$

where n,m are discrete time idices, g is the original image cut, d is distortion, and x is the resulting noisy cut

4. In the frequency domain for frequency indices k,l:

$$X_{k,l} = G_{k,l} + D_{k,l} \quad (9)$$

5. Spectral subtraction [9]:

$$\hat{G}_{k,l} = \begin{cases} (|X_{k,l}| - \alpha\, |\hat{D}_{k,l}|)\ e^{j\, arg\{X_{k,l}\}} & \text{for } \alpha\, |\hat{D}_{k,l}| \le |X_{k,l}| \\ 0 & \text{otherwise} \end{cases} \quad (10)$$

where $\hat{D}_{k,l}$ and $\hat{G}_{k,l}$ are the spectral estimates of noise and the recovered image, resp.

6. Optimation of α - the maximum of the signal to noise ratio (SNR) (see Fig. 7):

$$SNR = 10 \cdot log_{10} \left(\frac{var[g(n,m) - x(n,m)]}{var[g(n,m) - \hat{g}(n,m)]} \right) \quad (11)$$

where $\hat{g}$ stands for the de-noised image

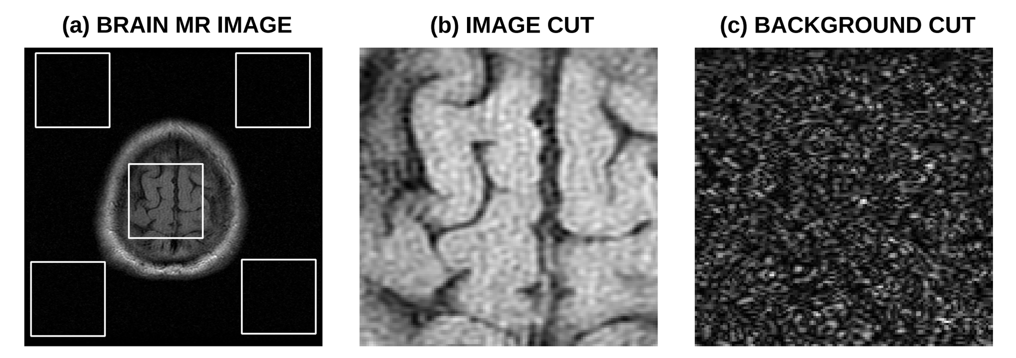

Fig. 6. Brain MR image cuts representing **(a)** axial plane brain MR image number 0, **(b)** a cut containing image information, and **(c)** one of the background cuts without any useful information

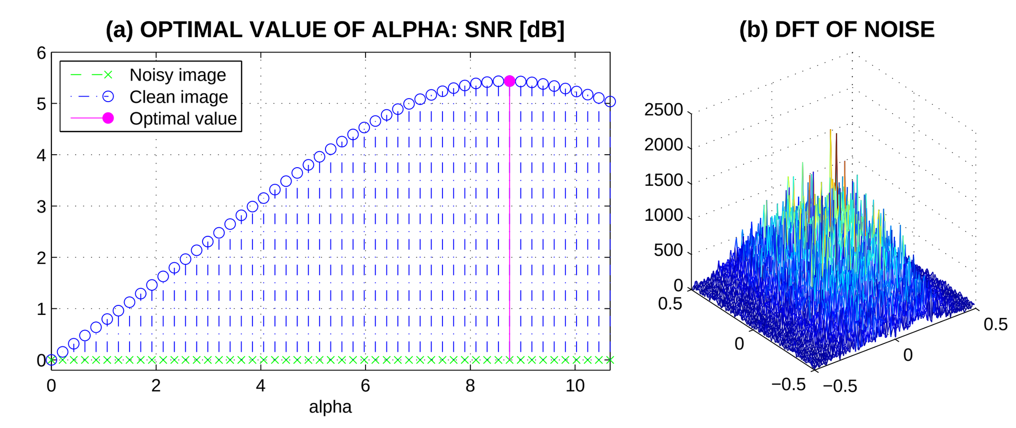

Fig. 7. Optimation of α displaying **(a)** dependence of the SNR [dB] on the value of α and **(b)** the magnitude Fourier spectrum of additional noise

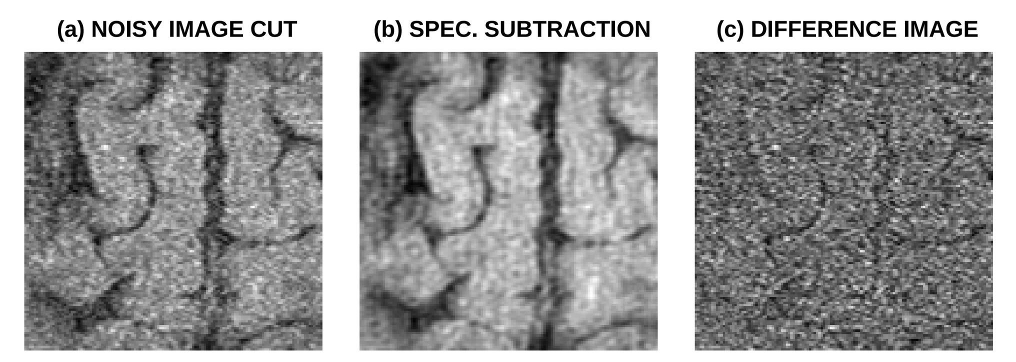

Fig. 8. Spectral subtraction standing for **(a)** the noisy image, **(b)** the image after spectral subtraction, and **(c)** the residual image enhanced for visual presentation

Conclusions

It is possible to conclude that the 3-D image de-noising can significantly improve results achieved by processing of individual images. Results presented in Table 2 summarize numerical experiments for real MR biomedical bodies using the Haar volumeric decomposition enabling also very simple reconstruction of the three-dimensional body.
As an alternative method of image de-noising, we present the Fourier transform utilised in spectral subtraction of magnitude spectra.
Our further studies will be devoted to the application of specific wavelet functions for volumetric enhancement of biomedical structures. The purpose of such a study is in the detection of image components and in visualization of general slices of the 3-D structures.

References

[1] A. Procházka and J. Ptáček. Wavelet Transform Application in Biomedical Image Recovery and Enhancement. In *The 8th Multi-Conference Systemics, Cybernetics and Informatic, Orlando, USA*, volume 6, pages 82–87. IEEE, 2004.

[2] E. Bullmore, J. Fadili, V. Maxim, L. Sendur, J. Suckling B. Whitcher, M. Brammer, and M. Breakspear. Wavelets and Functional Magnetic Resonance Imaging of the Human Brain. *NeuroImage*, 23(Sup 1):234–249, 2004.

[3] C. Zhang and H. X. Zheng and D. B. Ge. 3-D Wavelet-Based Multiresolution Analysis. In *Proceedings of the 5th International Symposium on Antennas, Propagation and EM Theory*, pages 301 – 304. IEEE, 2000.

[4] D. Montgomery and F. Murtagh and A. Amira. A Wavelet Based 3D Image Compression System. In *Proceedings of the Seventh International Symposium on Signal Processing and Its Applications*, volume 1, pages 65 – 68. IEEE, 2003.

[5] G. Menegaz and L. Grewe and J. P. Thiran. Multirate Coding of 3D Medical Data. In *Proceedings of the 2000 International Conference on Image Processing*, volume 3, pages 656 – 659. IEEE, 2000.

[6] J. Wang and H. K. Huang. Medical Image Compression by Using Three-Dimensional Wavelet Transform. *IEEE Transactions on Medical Imaging*, 15(4):547 – 554, 1996.

[7] N. Kingsbury. Complex Wavelets for Shift Invariant Analysis and Filtering of Signals. *Journal of Applied and Computational Harmonic Analysis*, 10(3):234–253, May 2001.

[8] D. E. Newland. *An Introduction to Random Vibrations, Spectral and Wavelet Analysis*. Longman Scientific & Technical, Essex, U.K., third edition, 1994.

[9] T. Kobayashi and T. Shimamura and T. Hosoya and Y. Takahashi. Restoration from Image Degraded by White Noise Based on Iterative Spectral Subtraction Method. *IEEE International Symposium on Circuits and Systems*, 6, 2005.

[10] Saeed Vaseghi. *Advanced Digital Signal Processing and Noise Reduction*. John Wiley & Sons, West Sussex, U.K., third edition, 2006.

15th International Conference

DSP 2007

Cardiff University, Wales, UK

1st – 4th July 2007